DIPOLE IDENTIFICATION OVER A CYLINDER SECTION IN SUBSONIC JET FLOW USING GENERALIZED INVERSE BEAMFORMING

Paulo A. G. Zavala, zavala@fem.unicamp.br
José Roberto de França Arruda, arruda@fem.unicamp.br
Computational Mechanics Department, UNICAMP, Campinas/SP, Brazil

Wim Desmet, wim.desmet@mech.kuleuven.be
Wim De Roeck, wim.deroeck@mech.kuleuven.be
PMA, Katholieke Universiteit Leuven, Belgium

Abstract. *Several efforts have been made in the field of aeroacoustics to understand sound generation and propagation. New experimental techniques have been applied in order to characterize the phenomena involved in these problems. In this work, the generalized inverse beamforming is used to identify the dipole distribution formed on top of a cylinder section in a subsonic air jet flow. The jet impinges asymmetrically on the cylinder, causing higher speeds on one side of the obstacle. This configuration could be representative for landing gear tire noise generation. The identification is validated through numerical cases. With the dipole distribution identified, equivalent pressure mappings are built and estimated directivity plot generated for the main plane of radiation.*

Keywords*: Beamforming, Aeroacoustics, Inverse Problems*

1. INTRODUCTION

The study of sound generated by air flow through obstacles has received attention since the establishment of the acoustics fundamentals, but it was subject of scientific scrutiny on the work performed by Strouhal in 1878, where tonal noise was observed in some particular flow conditions over slender objects. This phenomenon was called Aeolian tones and is still object of investigation by important research centers, for example, as illustrated by King on his work on 2009, where several obstacle profiles were subjected to flow speeds on the range of Mach 0.1 to 0.2. Evaluations of Strouhal frequencies and sound-pressure levels relationships were obtained and commented for different diameters and length characteristics.

Several efforts have been made also on the prediction of sound generation on these problems, for example, Takaishi in 2007, presented the source regions based on vortex sound theory close to the flow separation regions. On this work, the acoustic mappings and directivity plots indicate a dipole radiation transversal to the flow for low frequencies, and aligned to the flow for higher frequencies. Another interesting work was presented by Martínez-Lera on 2007 using Curle's Analogy from 1955, where again, the dipole like radiation pattern is obtained cross to the flow direction. Similar results were also obtained by numerical analysis by Guasch and Seo in 2007, and Müller in 2008, obtaining by different methods the dipole like directivity cross to the flow.

Efforts on the experimental side to the identification of generated sources normally are restricted to the localization of the radiation centers. Highly considered methods like Clean-SC and DAMAS, presented by the works of Sijtsma in 2007, and Brooks in 2004, respectively. Damas was revised by Dougherty in 2005 (DAMAS2), and by Brooks in 2006 to include spatial source coherence (DAMAS-C). Both methods, Clean-SC and Damas are widely used on the field to characterize aeroacoustic sources, however these methods are normally based on monopole type of radiation, restricting the results analysis in terms of directivity, for example.

In 2008, Suzuki proposed a method based on the microphone array cross-spectral matrix eigen-structure, and the solution of an inverse problem, the Generalized Inverse Beamforming. This method enhanced the dynamic range on the sources detection compared to the conventional beamforming, allowing it also to be used on dipole identification. Other advantages are the possibility to identify coherent and incoherent simultaneous source regions, for concentrated as well for distributed source regions.

In 2010, the method was applied for the identification of dipole sources on the same problem presented in this work, subsonic jet flow over a cylinder section. On that work, the identification was performed on peak emissions events, allowing the identification of fluid separation regions as well the main directions of radiation through the equivalent pressure mappings generated by the identified sources. In this paper, the generalized inverse beamforming is applied on the full measurement data set to obtain the identification of a representative dipole source distribution and orientation for the main frequency of radiation.

The paper starts with the main concepts on the generalized inverse beamforming, as long as the convection and refraction modeling adopted. The testing details are presented and numerical investigation is performed to illustrate the identification capabilities for the chosen frequency. Equivalent pressure mappings are presented for the main radiation plane, according to the identified source distributions, and in the end, the directivity plot is showed and discussed.

2. GENERALIZED INVERSE BEAMFORMING

The method proposed by Suzuki in 2008 starts from the Cross-Spectral Matrix (CSM), here adopted as *R*, created based on the array microphone spectrums:

$$\left(\overline{q}\,\overline{q}^{H}\right) = R \tag{1}$$

where $\overline{q}$ is the averaged spectrum matrix and $\overline{q}^{H}$ represents the complex conjugate transpose. To keep consistency between spectrums averaging, one microphone is kept as phase reference.

Since the CSM is non-negative definite and Hermitian, it can be decomposed on its eigenvalues and eigenvectors:

$$R = U\Lambda U^{H} \tag{2}$$

where U is the eigenvector matrix and Λ is the eigenvalue matrix.

Each eigenvalue is related to a coherent source distribution, and the eigenvector represents the array response to this coherent source distribution. The number of significant eigenvalues represents the number of significant coherent source distributions, while the least eigenvalues are related to incoherent noise.

After retrieving the number of eigenvalues and eigenvectors that represent the relevant source distributions detected by the array of sensors, it is possible to define the i^{th} eigenmode as:

$$v_i = \sqrt{\lambda_i}\,u_i \tag{3}$$

where v_i is the i^{th} eigenmode; λ_i is the i^{th} eigenvalue; and u_i is the i^{th} eigenvector.

The noise source localization problem can be formulated as finding the source vector, a_i, that solves the following equation:

$$Aa_i = v_i \tag{4}$$

where A is the transfer matrix with possible source types; and a_i is the i^{th} source strengths vector.

The transfer matrix contains the radiation patterns from each target grid point to every sensor position. The transfer matrix used in this work consists of a distribution of dipole sources.

The radiation for a dipole considered in this work is based on the second spherical harmonic, and can be described, using the same formulation as adopted on Suzuki, 2008, without convection or refraction, as:

$$p = \frac{a_{dip}c_{dip}}{4\pi r}\frac{\vec{r}\cdot\vec{v}}{r^2}(-1+jkr)e^{-jkr} \tag{5}$$

where p is pressure; a_{dip} is the dipole strength; c_{dip} is the dipole coefficient; r is the distance from source to a microphone; $\vec{r}$ is the vector from target grid point to array microphone location; $\vec{v}$ is the dipole orientation vector; and k is the circular wavenumber.

Suzuki adopted a coefficient to normalize the identified dipole strength to unity, since the dipole presents a lower radiation efficiency, $c_{dip} = \sqrt{|r_{M.C.}|/(kr_{aper})}$, where $r_{M.C.}$ is the microphone array centroid and r_{aper} is the array aperture diameter.

In order to solve eq. (3) the generalized inverse or the pseudo-inverse is used to calculate the source vector. An underdetermined system is obtained when a larger number of grid points than sensors are used:

$$a_i \approx A^{H}(AA^{H})^{-1}v_i \tag{6}$$

In the case of an overdetermined system, the following equation can be used:

$$a_i \approx (A^{H}A)^{-1}A^{H}v_i \tag{7}$$

Since the matrix AA^H is usually ill-conditioned, the Tikhonov regularization is adopted to solve equation (6) or (7). This introduces an artificial additive diagonal term on this matrix, improving its condition, thus resulting in the following equations for the underdetermined and the overdetermined formulations, respectively:

$$a_i \approx A^H (AA^H + \alpha^2 I)^{-1} v_i \tag{8}$$

$$a_i \approx (A^H A + \alpha^2 I)^{-1} A^H v_i \tag{9}$$

where I is the identity matrix.

The Tikhonov regularization corresponds to the minimization of the following cost function:

$$J_2 \equiv \|a_i\|^2 + \alpha^{-2} \|v_i - A a_i\|^2 \tag{10}$$

where $\|\cdot\|$ is the Euclidean norm; α is the Tikhonov regularization factor.

According to Suzuki, the square of the regularization factor could be adopted as a fraction of the greatest eigenvalue of the matrix AA^H, with suggested range from 0.1% to 5%. However, the solution brought by equations (8) and (9) is a least squares approximation, and the use of a least squares approach does not lead directly to the source vector with minimum L-1 norm. More accurate distributed source strength can be calculated in an iterative process, which is adopted to find the solution that minimizes a more appropriate cost function:

$$J_1 \equiv |a_i| + \alpha^{-2} |v_i - A a_i|^2 \tag{11}$$

where $|\cdot|$ is the L-1 norm, representing the direct summation of the vector terms.

This new minimization problem presents the advantage of more accurate overall strength estimation for distributed sources. However, since no direct approach can be adopted to solve this problem, the method used in this work searches for the minimization of the J_1 cost function iteratively, truncating the source vector terms, or grid points, that are less relevant, and using the least squares equation to recalculate the source vector. A simplified version of the algorithm can be described as:

1) Calculate initial source vector, a_i, using generalized inverse equations (8) or (9);
2) Reorder and truncate (10%) the source vector, discarding the smallest terms;
3) Calculate a new source vector, using equations (8) or (9);
4) Repeat items 2 and 3 until a pre-defined number of source terms is reached;

3. CONVECTION AND REFRACTION MODELING

The free-field dipole radiation equation shown in (5) is no longer representative in the case of a source in flow condition. With the observer outside the flow, the refraction representing the interaction of the outcoming radiation waves from the sources on the boundary shear layer has to be taken into account. These can be done in a simplified approach using the modeling presented by Amiet in 1975 as suggested in Mueller (Ed.), 2002.

The simplified modeling consists of a source at the center of a cylindrical tubular jet profile, and the propagation to the outside observer is treated as a 2D problem. Figure 1 illustrates the relationship between the emission direction, the convection direction, and the refraction direction according to this modeling.

Equation (12) below shows the relationships between these directions:

$$R_m \cos\theta_m = R_t \cot\theta + (R_m \sin\theta_m - R_t)\cot\theta_0 \tag{12}$$

where R_m is the distance from the source to the microphone; θ_m is the angle formed from the source to the microphone; R_t is the shear layer distance to the center of the cylindrical flow; θ is the propagation angle in flow and θ_0 is the angle from the shear layer to the microphone.

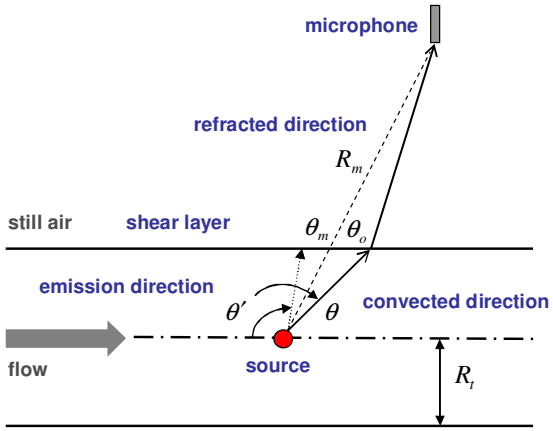

Figure 2. Convection and refraction modeling based on Amiet, 1975.

4. EXPERIMENTAL TEST DETAILS

The test setup is the same used on Zavala, 2010, and can be observed on figure 3, along with the array used on this test. The adopted array consists of a 6-arm spiral configuration based on the Underbrink multi-arm spiral design, with 30 microphones. The array has 1m aperture and is positioned at 1.25m from the jet axis. The circular cylinder section is 40mm in diameter, and 20mm in length. The cylinder is positioned 0.4m from the outlet pipe. The array center is aligned with the cylinder center. Details can be observed in figure 4. The array microphone positions and target grid points can be seen in figure 5.

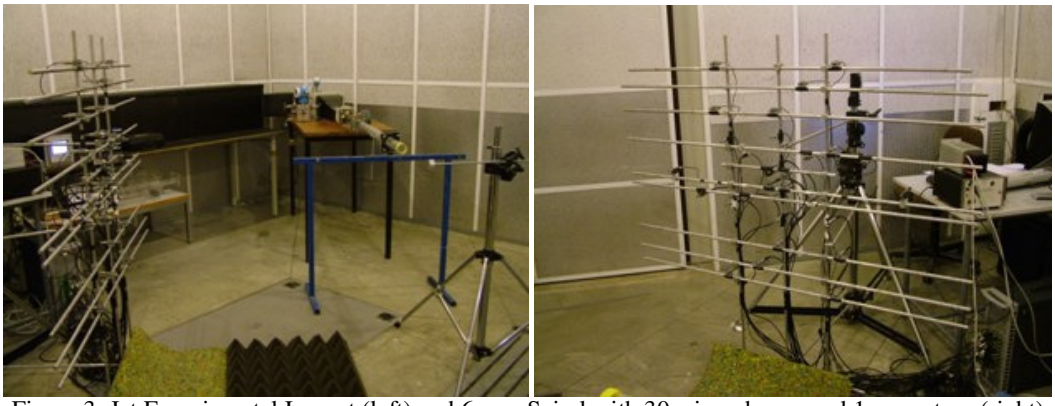

Figure 3: Jet Experimental Layout (left) and 6-arm Spiral with 30 microphones and 1m aperture (right)

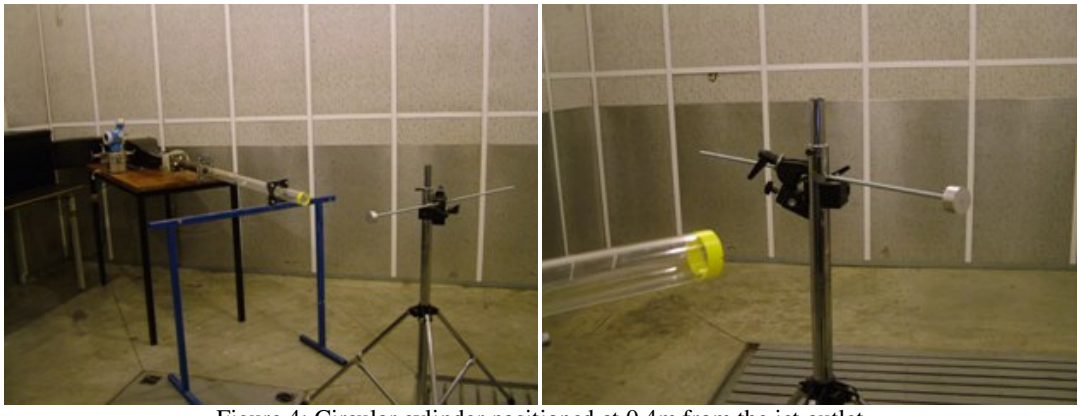

Figure 4: Circular cylinder positioned at 0.4m from the jet outlet

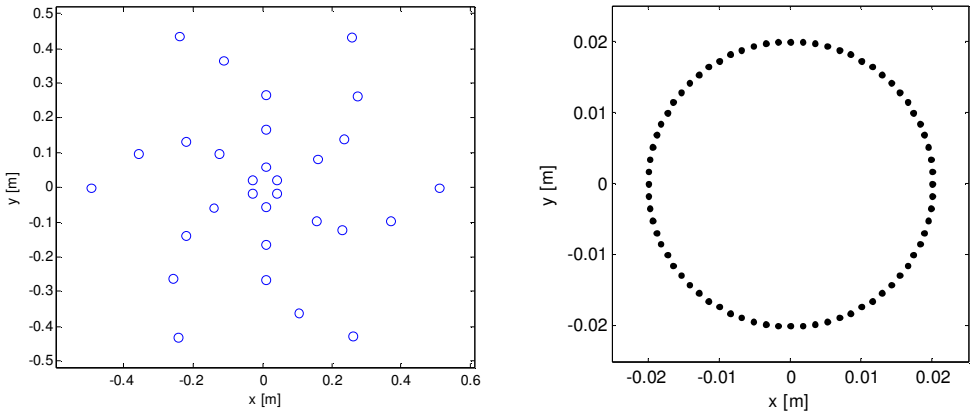

Figure 5: Array 6-arm spiral microphone positions (left) and target grid points (right)

The target grid consist of 72 points, 5 degrees interval, distributed over the x-y plane. The jet axis is positioned with approximately 2 degrees of inclination, and this produced a non-symmetric speed profile. The measurements are done with a flow speed at the outlet pipe of approximately 0.2M, and a hot wire measurement without the cylinder is presented in figure 6.

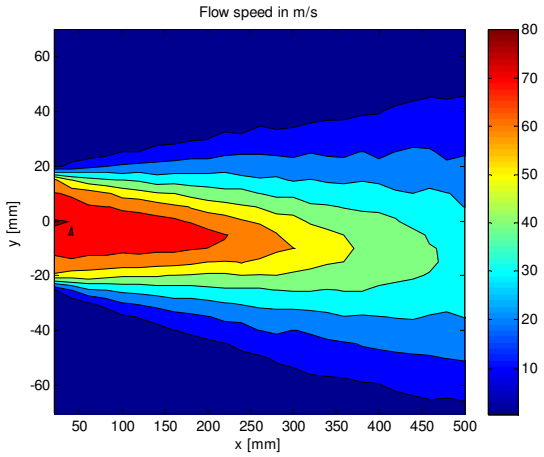

Figure 6: Jet speed hot wire measurement results in x-y plane

The x-y plane is at the jet axis and parallel to the array. The estimated flow speed at the cylinder position (x=400mm) is adopted as 0.07M, and refraction shear layer is estimated at 40mm from the jet axis, those are simplifications to the real situation, where the jet flow is deflected and produces more complex refraction around the cylinder.

The cylinder section dimensions were chosen to produce a concentrated source region, almost compact, to help the identification effort by the proposed method. However, the ratio between the diameter and length, on this case, 2, already indicate that a tonal noise would not be observed, and more broadband random character would be observed.

Using a 102.4kHz sampling acquisition system, spectrums can be built using blocks with 10240 samples, and frequency resolution of 10Hz. The microphones spectrums amplitude averaging over approximately 4 seconds is presented on Fig. 7. The averaging used 100 spectrums and approximately 60% overlap. This graph would represent the most important frequency emissions, and the peak is detected at 370Hz. This frequency is then chosen for the investigation.

5. NUMERICAL INVESTIGATION ON IDENTIFICATION PERFORMANCE

Before applying the identification directly to the experimental data, a simulation is build with objective to verify if the method is able to separate and identify source regions considering that the obstacle in quite small compared to the wavelength for 370Hz emission.

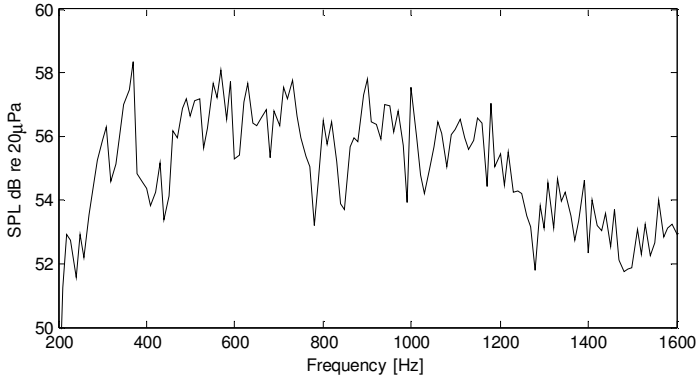

Figure 7. Amplitude averaging of microphones spectrum.

Two cases are adopted, the first with dipoles uniformily distributed from 45° to 90°, and the second from 270° to 315°, both with normal to the cylinder surface orientation and in the x-y plane. The identification is performed with artificial noise added to the CSM, similar to the strategy adopted in Suzuki 2008. The iteration stop criteria is adopted as to reach ¼ or less of the grid points, and iterations stopped with 16 source terms. Identification results are presented in Fig. 8. Arrows are adopted to represent dipoles strength and orientation on the x-y plane.

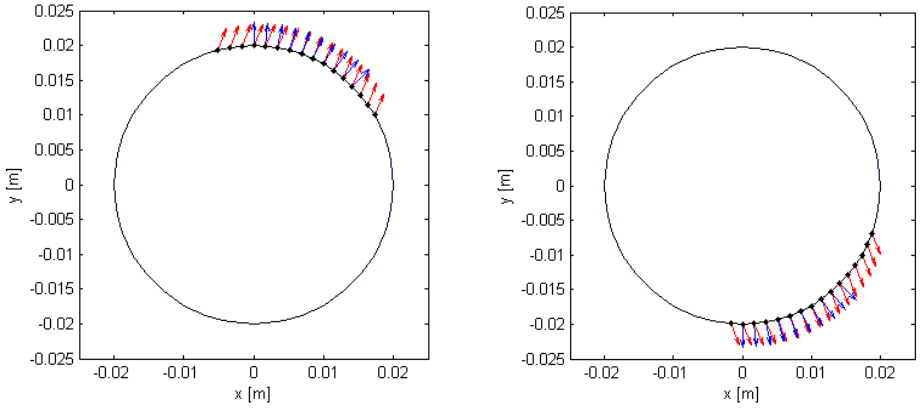

Figure 8. Dipole identification verification results on case 45° to 90° (Left) and 270° to 315° (Right). Arrows represent dipoles: blue (numerical source); red (identification results).

The results shows good agreement on the general location of the dipole distribution despite the region size compared to the wavelength. However, the identification results seem to adopt a general orientation, not being able to capture the small orientation changes in the source region. Even though those results can be considered satisfactory for the main objective on this work that is to characterize the main source regions and general orientations on those regions.

6. EXPERIMENTAL IDENTIFICATION RESULTS

Using the same strategy for the spectrums averaging, 100 spectrums over 4 seconds (60% overlap), using one microphone in the array inner circle as reference for the averages, the CSM is built and the identification performed. Stop criteria is chosen again as to reach ¼ grid region, keeping in the end, 16 source points. The dipole identification results can be observed on Fig. 9. Contrary to the objective in Zavala, 2010, where the identification is performed in a single peak event, the averaging would represent an overall estimation in location and orientation for that particular frequency. The identification is performed to assess the dipole orientation on the x-y plane only.

The result shows two regions of distributed dipoles, with similar orientations, close to vertical direction. Considering that the flow impinges the cylinder section asymmetrically, with higher speeds on the bottom area, the regions of

separation of fluid is in accordance to the expected flow speed profiles. The pressure fluctuations due to these separations would be the main influence on the source region generation. These locations and orientation are in accordance to the work of Takaishi, 2007, even considering that in this paper, the flow is slightly asymmetric and the cylinder diameter to section length ratio is smaller, may causing other 3D effects on source location.

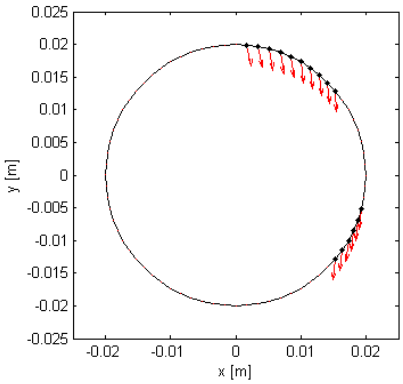

Figure 9. Dipole identification using experimental data

With the identification results showed in Fig. 9, Equivalent Pressure Mappings can be generated for the main plane of radiation, x-y plane, shown in Fig. 10.

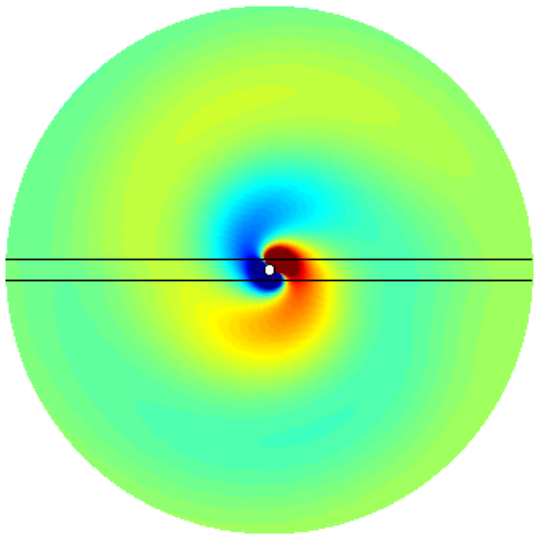

Figure 10. Equivalent Pressure Mapping with 1m radius. Horizontal lines represents the shear layer simplification.

The distributed dipole configuration with two regions and similar orientations leaded to a spiral like type of propagation, not presenting a clear radial zero-pressure intermediate region between the two dipole main directions of emission. This interesting result is confirmed if a smaller dynamic range is adopted for the visualization of the same result, shown in Fig. 11.

This kind of radiation pattern can also be observed in dipoles subjected to rotation, which indicates that one possible interpretation of the result is that the captured dipole radiation using the averaging in fact would correspond to a rotating dipole radiation, which was not observed on Zavala, 2010 work, using a single event identification. This difference could be explained considering that for one particular emission, the oscillations in pressure are normally instantaneously symmetric in respect of top and bottom regions for cylinder in flow simulations and acoustic radiation. The averaged identification represent not only the dipole main direction, cross-flow, but also the change in phase between the bottom and upper regions.

In order to investigate the main radiation directions, the directivity is build according to the definition from Kinsler, 1982, shown in Fig. 12.

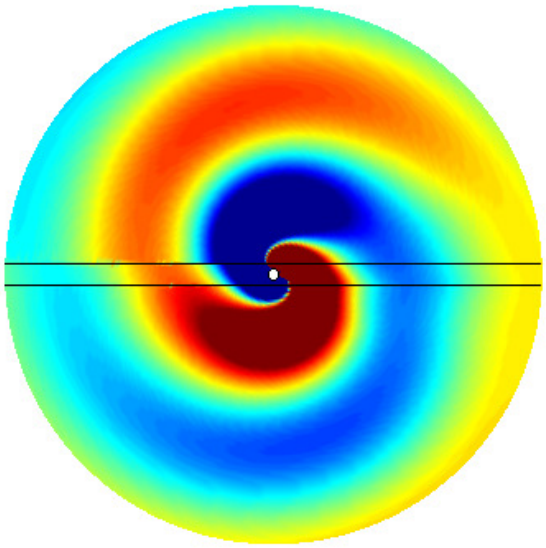

Figure 11. Equivalent Pressure Mapping for 1m radius (reduced dB range)

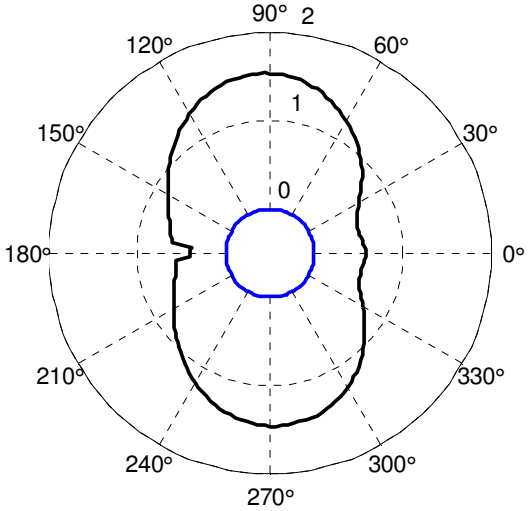

Figure 12. Directivity plot calculated at 1m radius in respect to the cylindrical equivalent radiation.

Despite the spiral like pressure mapping for the identified dipole distributions, the directivity confirms the cross-flow expected orientation for low frequencies, as mentioned in Takaishi, 2007. The directivity seems to deviate according to the low asymmetry on the flow (2°), with higher speeds on the bottom of the cylinder.

The regions around 0° and 180° shows the convection effects, since they are on the flow region. The spiral like radiation causes still important radiation even close to 90° from the main radiation directions.

6. CONCLUSIONS

This paper presented a new approach to the aeroacoustic sources identification, localization and characterization, such as dipole distributions over compact obstacles in subsonic jet flows. Microphone spectrums averaging leaded to different results when compared to single event identifications presented in a previous work. The spiral like radiation pattern suggests that the dipole would be rotating, despite that no rotation is considered on the transfer matrix modeling. This rotation in fact would be the representation of the pressure oscillation between the two identified regions.

The directivity obtained on the experimental setup is in fully agreement with the numerical cases studied in literature, even considering that those problems differs in diameter/length ratio to the tested obstacle.

7. ACKNOWLEDGEMENTS

The first author is grateful for his research stay at the Katholieke Universiteit Leuven (Belgium) at the PMA department as a collaboration effort with the Computational Mechanics Department of the State University of Campinas (UNICAMP/Brazil), supported by a fellowship received from the Marie Curie EST SimVia2 Program and regular PhD student scholarship in 2009 and 2010. This work is also supported by a PhD student scholarship from FAPESP/SP/Brazil in 2011.

8. REFERENCES

Amiet, R. K., 1975. "Correction of open jet wind tunnel measurements for shear layer refraction". AIAA paper 75-532.

Brooks, T.F. and Humphreys, W.M., 2004. "A deconvolution approach for the mapping of acoustic sources (DAMAS) determined from phased microphone arrays". Journal of Sound and Vibration, Vol. 294, March 2006, pp. 856-879, also AIAA paper 2004-2954, May.

Brooks, T.F. and Humphreys, W.M., 2006. "Extension of DAMAS phased array processing for spatial coherence determination (DAMAS-C)", AIAA paper 2006-2654, May.

Curle, N. 1955. "The influence of solid boundaries on aerodynamic sound". Proc. R. Soc. London, Ser. A 231, 505-514. 216-251.

Dougherty, R. P., 2005. "Extension of DAMAS and benefits and limitations of deconvolution in beamforming". AIAA paper 2005-2961.

Guasch, O. and Codina, R. 2007. "An algebraic subgrid scale finite element method for the convected Helmholtz equation in two dimensions with applications in aeroacoustics". Comput. Methods Appl. Mech. Engrg. 196 4672-4689.

King, W. and Pfizenmaeir, E., 2009. "An experimental study of sound generated by flows around cylinder of different cross-section". Journal of Sound and Vibration, Ed. Elsevier, 328 318-337.

Martínez-Lera, P., Pradera, A. and Schram, C., 2007. "Efficient implementation of equivalent sources from CFD data in Curle's Analogy". 13th AIAA/CEAS Aeroacoustics Conference (28th AIAA Aeroacoustics Conference), 2007-3569.

Mueller (Ed.), T. J., 2002. "Aeroacoustic Measurements". Springer, New York.

Müller, B. 2008. "High order numerical simulation of Aeolian tones". Computers and Fluids, 37 450-462.

Seo, J. H. and Moon, Y. J. 2007. "Aerodynamic noise prediction for long-span bodies". Journal of Sound and Vibration, 306 564-579.

Sijtsma, P. 2007. "CLEAN based on spatial source coherence". 13th AIAA/CEAS Aeroacoustics Conference (28th AIAA Aeroacoustics Conference), 2007-3436.

Strouhal, V. 1878. "Über eine besondere art der Tonerregung". Annalen der Physik und Chemie (Leipzig) Series 3 (5)

Suzuki, T., 2008. "Generalized Inverse Beam-forming algorithm resolving coherent/incoherent, distributed and multipole sources". 14th AIAA/CEAS Aeroacoustics Conference (29th AIAA Aeroacoustics Conference), 2008-2954, May.

Takaishi, T., Miyazawa, M. and Kato, C., 2007. "A computational method of evaluating noncompact sound based on vortex sound theory". J. Acoust. Soc. Am. 121 (3), March

Zavala, P.A.Z., De Roeck, W., Janssens, K., Arruda, J.R.F., Sas, P., Desmet, W., 2010. "Aeroacoustic source identification using generalized inverse beamforming". ISMA 2010 paper ID 672, Leuven, Belgium.